BB

CEA/SACLAY
DSM

Sw9743

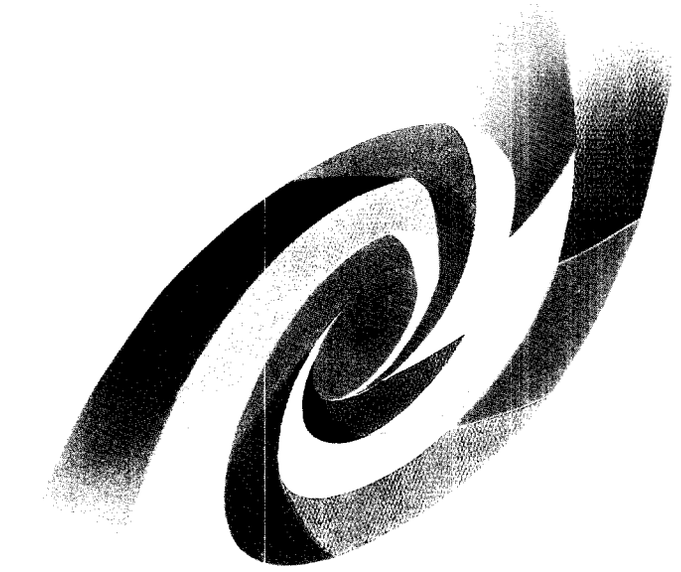

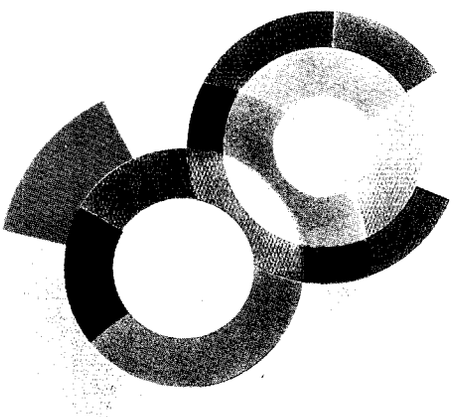

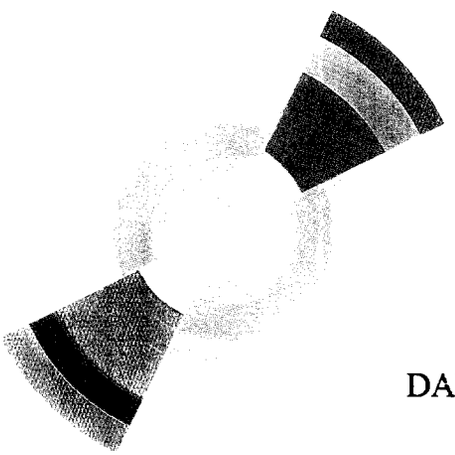

DAPNIA/SPhN-97-21 03/1997

Boiling a nucleus

DAPNIA

E.C. Pollacco, J. Brzychczyk, C. Volant, R. Legrain, L. Nalpas,
D.S. Bracken, H. Breuer, R.G. Korteling, K. Kwiatkowski,
K.B. Morley, E. Renshaw Foxford, V.E. Viola, N.R. Yoder,
J. Gomez del Campo and J. Cugnon

Département d'**A**strophysique, de Physique des **P**articules, de Physique **N**ucléaire et de l'**I**nstrumentation **A**ssociée
CEA/Saclay F-91191 Gif-sur-Yvette Cédex

Couverture Sylvie Cabrit et Marc Sauvage

XXXVth International Winter Meeting on
Nuclear Physics,
BORMIO, Italy, 3-8 February 1997

Boiling a nucleus†

E. C. Pollacco[1], J. Brzychczyk[1,3], C. Volant[1], R. Legrain[1],L. Nalpas[1]
D.S. Bracken[2] ,H. Breuer[5], R.G. Korteling[4], K. Kwiatkowski[2],
K.B. Morley[2], E. Renshaw Foxford[2], V.E. Viola[2],N. R. Yoder[2],
J. Gomez del Campo[6] and J. Cugnon[7]

[1] CEA DAPNIA/SPhN, CE Saclay, 91191 Gif-sur-Yvette CEDEX, France.
[2]Dept. of Chem. & IUCF, Indiana Univ., Bloomington, IN47405, USA.
[3]Inst. of Phys., Jagiellonian Univ. 30-059 Krakow, Poland.
[4]Dept. of Chem., Simon Fraser Univ., Burnaby, BC, Canada.
[5]Dept. of Phys., Univ. of Maryland, College Park, MD 20742, USA.
[6]Oak Ridge National Laboratory, Oak Ridge, TN37831,USA.
[7]Univ. de Liège, Inst. de Physique, B-4000 Liège 1, Belgium.

INTRODUCTION

As with a number of papers presented at this XXXV Bormio conference , this study considers how nuclei respond to large amounts of thermal energy. By *large* we have in mind values reaching the total nucleon binding energy, B. By *respond* we refer, for example, to the trajectory that the system traces in a density versus temperature plot[1]. For a nucleus of mass 130 and low excitation energy, $E^* \sim 100$ MeV, the density is constant and the temperature is dissipated entirely by evaporation. With increasing E^*, evaporation yield gradually gives way to fission and then to multifragmentation [2]. Multifragment production is believed to occur once the nucleus reaches low density. The question that is addressed in this work is whether the *evaporative* channel is still present at high E^*. More specifically, we set out to detect events with a single residual heavy fragment, HF, accompanied preferentially with light particles at $E^* \sim B$. and to compare the data with evaporative decay [3]. At such energies multifragment and suedo-fission production are calculated to be dominant [2]. It is therefore conceivable that the *evaporation* chain is modified by the strong presence of the other channels. For example if we suppose that at high temperatures a monopole expansion [4] occurs, then HF could be associated with events with a monopole collapse. Therefore a signature might still persist in the particle emission chain for the events of interest. This work is interesting within the context of ref. 5.

† Experiment performed at the Laboratoire National Saturne, France

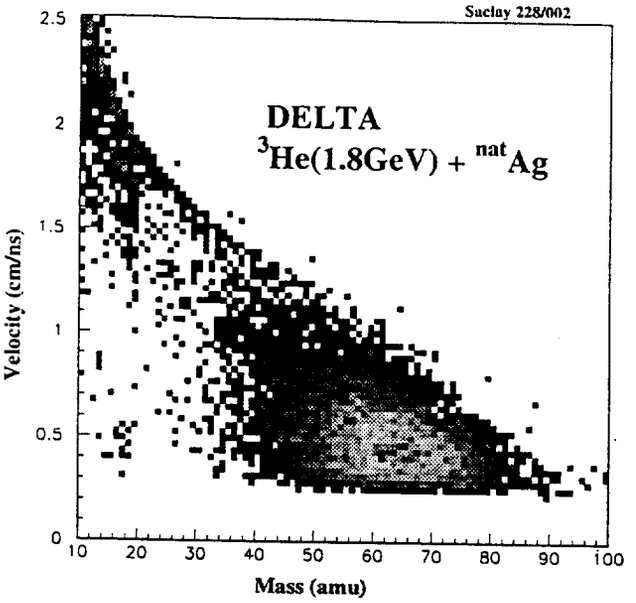

Figure 1. Residual mass versus velocity plot.

experimental set-up consisted of four parts. (i) To measure leading protons ARCOLE was used[14]. This consists of a forward plastic wall made up of 28 fast plastics and mounted so as to have a hole in the centre for the beam. Light from each plastic was read out by two photomultipliers. This assembly covered an angular range of approximately 2.5 to 12° and was positioned to give a minimum flight path from the target of 4 meters. (ii) To detect heavy fragments, HF, a circular hodoscope, DELTA, which included 30 high field Si detectors was used. The target-detector flight path was 60 cm and covered angles between 5 to 10°. (iii) Light charged particles ($Z \leq 2$), LCP, and intermediate mass fragments ($Z \leq 20$), IMF, were detected in an array called ISiS[12,15] which contains 162 triple detector telescopes in a tight geometry. Each telescope is composed of a gas-ionisation chamber, a fully depleted 500μm ion-implanted silicium detector and a 28 mm CsI(Tℓ) crystal. The geometrical acceptance is 70% and thresholds are better than 1 MeV.A. The charge, Z, resolution ranged up to 20. Mass resolution is obtained for those particles which punch through the Si crystal. (iv) An active collimator assembly was employed to vetoe the beam halo particles reaching or stopping in ISiS.

Data Analysis

Fig. 1 gives the superimposition of 26 mass vs. velocity plots from DELTA for fragments with a minimum trigger of two particles in ISiS. The mass was computed from the time between DELTA - ISiS and energy measurements. Corrections due to time delay[16] and energy defect[17] were included. The latter was achieved through a coincident set-up with slowed down fission fragments in a separate measurement. Velocity thresholds were all better than 0.25 cm/ns. We remark that in light ion

we refer to thermal mass and charge. To compute the thermal quantities the principal corrections which were introduced are (i) the detector acceptance. This includes the efficiency as a function of charge and mass for low energy particles. The efficiency corrections were established with the aid INC + SIMON and the detector filter. (ii) By far the largest addition to the excitation energy is the contribution of the neutron energy. The mean energy per neutron K_n as a function of E^* was calculated using the code LILITA [19]. An iterative procedure was used. (iii) To obtain the total mass and charge per event, the mass (charge) of the IMFs (HF) was read off from a table of mass versus charge which takes into account the evaporation process. (iv) The thermal quantities were calculated by summing over the particle kinetic energy, mass, charge and Q-values (Q_i) event-by-event. In this analysis the sum was carried over heavy residue and all IMFs. For LCPs the sum was extended over particles with kinetic energies, K_i which are below (25, 32, 39, 54 and 61 MeV) for p, d, t, ^{3}He and ^{4}He respectively. The thermal charge, Z_{th}, gives the total mass, A_{th} by assuming an Z_{th}/A_{th} in the valley of stability. Subtracting the total detected mass from A_{th} gives the number of thermal neutrons, N_n. The energy, E_{th} was calculated by computing the sum $(N_n(K_n+Q_n) + (\Sigma(K_i+Q_i))$ over the thermal particles and corrected for the efficiencies. This analysis shows a constant $A_{th} = 92$ amu with E^* for values greater than 250 MeV and consistent with the INC calculations. Therefore a second and adopted method was also developed where A_{th} and Z_{th} are assumed and given by the INC calculations. In this case the efficiency correction was not employed and the missing mass and charge and corresponding energies were assumed to arise only from LCPs in the same proportion as the detected particles in the event. Performing simulations with the above described procedures shows that the E^* given by INC is well reproduced by the using a constant A_{th}. The efficiency method tends to give large widths in the E_{th} observable.

Results

In fig. 3 a plot is given of the detected heavy mass in DELTA as a function of $\epsilon^* = E_{th}/A_{th}$ with the IMF multiplicity, $M_{IMF} = 0$. We note a number of features. The largest yield is for events with mass of approximately 65. Higher masses are not detected with full efficiency due to the target thickness and energy threshold in DELTA as noted earlier. The island at high excitation $\epsilon^* \sim 9$ A.MeV is not considered here and correspond to events where the HF is not detected in DELTA. The line traced from low to high excitation represents the simulation trend. As shown the data stretch is well reproduced. The rectangle is drawn to have a centre at ϵ^*/B corresponds to 80% . The width and height of the rectangle represent the full width at half maximum for the mass and ϵ^* resolution respectively. The latter value was extracted using the INC+SIMON+FILTER simulation. For events in this region of ϵ^* =6-8 A.MeV the fraction of events with M_{IMF} greater than zero in this region is approximately 25%. These IMFs have charge distribution with a maximum at 3 and decaying very rapidly. This suggests that the loss of mass from the HF by IMF emission is not significant.

Considering the same representation as fig. 3 but with condition M_{IMF}=1 and 2 shows essentially the same data trend but with decreasing statistics and an increasing shift to lower residual mass with M_{IMF} . However no shift to high ϵ^* is remarked. In other words, inclusion of all IMF multiplicities does not change significantly the high

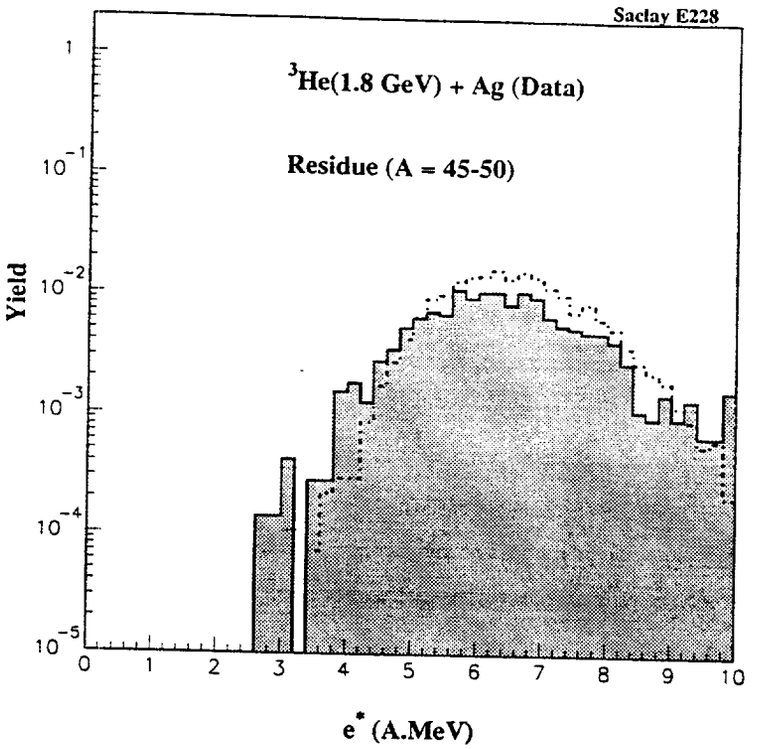

Figure 4. Experimental ϵ^* spectrum with the indicated mass window. The dashed curve represents the simulation.

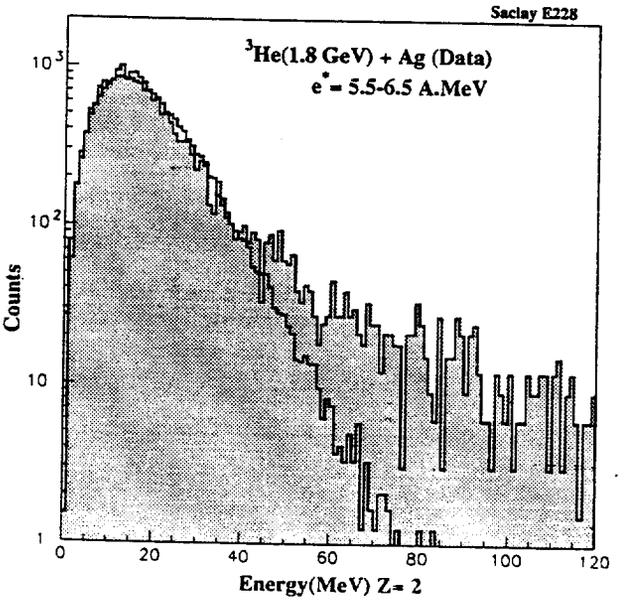

Figure 5. Energy spectrum for Z=2 in coincidence with HF for ϵ^* =5.5 - 6.5MeV/A.

7. M. Colonna, J. Cugnon and E. C. Pollacco, Phys. Rev. March(1997).
8. J. Cugnon, Nucl. Phys. A462, 751(1987).
9. Modified version of SIMON, D. Durand, Nucl. Phys. A541, 266(1992).
10. R. J. Charity et al., Nucl. Phys. A476, 516 (1988).
11. A. Botvina, A. S. Iljinov and I. Mishustin, Nucl. Phys. A507, 649(1992).
12. K. Kwiatkowski, contribution to this conference.
13. K. B. Morley et al., Phys. Lett. B355, 52(1995).
14. Y. Terrien et al., Phys Lett. B294, 40(1992).
15. K. Kwiatkowski et al., Nucl. Instr. Meth. A360, 5(1995).
16. S.B. Kaufman, et al., Nucl. Instr. Meth. 115, 47(1974).
17. H.O. Neidel, H. Henschel, Nucl. Instr. Meth. 178, 137(1995).
18. S.B. Kaufman and E. P. Steinberg, Phys. Rev. C22, 167(1980)
19. J. Gomez del Campo et al., Phys. Rev. C41 2689(1991)
20. S. Leray, J. de Phys. C4 275(1986).